PHOTOMETRIC DATA FOR THE OLD GALACTIC CLUSTER NGC 188

ALLAN SANDAGE
Mount Wilson and Palomar Observatories
Carnegie Institution of Washington, California Institute of Technology
Received September 18, 1961

ABSTRACT

Photoelectric and photographic data for about 500 stars in and near the galactic cluster NGC 188 are reported. The color-magnitude diagram suggests that NGC 188 is the oldest galactic cluster isolated so far The main-sequence termination point is about 1 mag. fainter than that of M67. Confirmatory spectroscopic evidence was obtained which shows that the stars in NGC 188 near the main-sequence turning point are 0 3 of a spectral class later than similar stars in M67.

The color-magnitude diagram for NGC 188 lies within 0.2 mag. of the lower envelope of the evolved part of the diagram for field stars near the sun Despite their great age, these old stars and the stars in NGC 188 appear to have nearly the same metal abundance as do the much younger Hyades stars. If this is so, then the enrichment of the heavy elements in the interstellar medium near the sun has been negligible in the disk of our Galaxy for most of the life of the disk. Analysis of the random photometric errors is given in Appendix A Comparison of the present data with the photometric results of Barkhatova is given in Appendix B.

I. INTRODUCTION

In the summer of 1948, Ivan King noticed that the galactic cluster NGC 188 was unusual in several respects. Not only is its galactic latitude high ($b^I = +23°$), but the cluster has a large angular diameter, even though the apparent magnitudes of its brightest stars are very faint. Either NGC 188 must be relatively distant (to account for the faintness of the stars) and therefore of large linear size, or the cluster is nearby, with more or less normal linear dimensions and with unusually faint absolute magnitudes for its brightest stars.

In 1956 Sidney van den Bergh (unpublished) obtained a preliminary luminosity function for NGC 188 by counting star images on the Palomar Sky Survey prints. He found that $\phi(M)$ for NGC 188 was similar to that of the high-latitude cluster M67, which is known to be old. Van den Bergh's result suggested that NGC 188 was a candidate for this rare group of old clusters. Photographic and photoelectric observations were begun with the 60-inch reflector in the winter of 1958 when the cluster was below the pole near lower culmination. These first photographic plates were measured by van den Bergh at the California Institute of Technology. His results established for the first time the nature of the color-magnitude diagram. Unfortunately, the pressure of van den Bergh's other work made it difficult for him to continue with the project. But it is to van den Bergh that credit must go for first showing that NGC 188 is similar to M67 and, therefore, that the cluster was worth a major observational effort.

Data to a very faint magnitude limit, better plates, and spectra were needed to establish that NGC 188 is as old as or older than M67. Observational work continued on the cluster through the observing seasons of 1959, 1960, and 1961.

II. THE OBSERVATIONS

Photoelectric measurements of 125 stars in and near NGC 188 were made with the 60- and 200-inch reflectors. The data are given in Table 1. Analysis of the internal consistency of the transfers of the U, B, V system to five local standards (stars I-106, II-29, III-4, III-136, and III-138) shows that the *mean* error of a single observation of the transfer is $\Delta V = 0^m.016$, $\Delta(B - V) = 0^m.012$, and $\Delta(U - B) = 0^m.027$. The average number of transfers to the U, B, V system for each of the five local standards was 13. The average number of separate nights when transfers were made was 8. Unless some

TABLE 1

PHOTOELECTRIC STANDARDS IN NGC 188

Ring I	V	B-V	U-B	n;60"	n;200"
8	16.52	0.72	0.27	-	1
31	16.31	0.78	0.32	-	1
44	16.41	0.75	0.31	-	1
47	14.98	0.73	0.23	-	1
48	14.90	0.71	0.36	1	1
49	15.71	0.70	0.19	-	1
50	13.88	0.47	-0.05	1	-
59	14.02	1.00	0.89	1	-
82	16.82	0.80	0.45	-	1
83	16.78	0.80	0.55	-	1
88	15.06	0.90	0.58	-	1
94	16.40	0.79	0.23	-	1
95	16.06	0.72	0.25	-	1
96	16.57	0.86	0.34	-	1
106	11.86	0.54	0.04	-	9
108	15.16	0.72	0.26	-	1
110	16.90	0.80	0.51	-	1
113	15.96	0.78	0.29	-	1
117	17.40	0.92	0.80	-	1
118	17.02	1.06	0.75	-	1
122	17.55	1.00	0.62	-	1
124	17.18	1.01	0.60	-	1
165	17.92	0.77	-	-	1
166	18.03	1.26	-	-	1
167	18.49	0.84	-	-	1
168	17.80	0.92	0.58	-	1
169	17.63	0.96	0.71	-	1
170	18.99	1.26:	-	-	2
171	18.72	1.03	-	-	1
172	19.07	1.30:	-	-	1
173	18.68	0.81	-	-	1
174	18.73	1.29	-	-	1
175	19.97	1.58	-	-	1
176	18.54	0.92	-	-	1
177	18.61	1.20	-	-	1
178	19.20	1.72	-	-	1
179	18.32	1.12	-	-	1
Ring II					
9	15.32	0.68	0.19	-	1
12	16.23	0.71	0.25	-	1
25	15.57	0.92	0.46:	1	1
27	15.29	0.68	0.19	2	2
28	15.85	0.64	0.18	2	1
29	9.58	0.50	0.01	2	14
43	15.87	0.73	0.21	-	1
46	13.37	0.52	0.11	2	5
47	13.49	0.63	0.05	1	-
51	12.96	1.18	1.12	1	1
55	15.43	0.66	0.20	-	1
67	14.93	0.74	0.24	-	1
72	12.41	1.34	-	1	-
73	15.03	0.69	0.19	-	1
75	10.84	1.28	1.34	1	1
76	12.38	1.18	1.02	1	-
80	15.69	0.69	0.16	-	1
82	14.21	0.46	-	1	-
91	16.29	-0.17	-1.00	-	2
93	15.01	0.82	0.42	-	1
95	12.54	0.76	0.36	1	1
112	16.16	0.72	0.23	-	1
113	16.52	0.84	0.44	1	-
115	15.89	0.71	0.21	-	1
116	16.05	0.70	0.23	-	1
121	16.28	0.70	0.25	-	1
130	16.72	0.81	0.23	-	1
131	16.36	0.74	0.30	-	2
177	16.04	0.74	0.28	-	1
*185	15.48	0.70	0.20	-	1

Ring II	V	B-V	U-B	n;60"	n;200"
201	17.53	1.04	-	-	1
202	17.28	0.84	0.60	-	1
211	17.42	0.94	0.63	-	1
212	17.20	0.91	0.74	-	1
223	17.56	1.08	-	-	1
224	17.64	1.20	-	-	2
231	17.76	1.09	0.90	-	1
233	18.11	1.12	-	-	1
234	18.04	1.19	-	-	1
Ring III					
1	15.51	0.69	0.20	1	2
2	15.59	0.58	-0.01	1	1
4	11.68	1.13	1.05	6	6
17	13.14	1.08	1.03	1	-
18	11.36	1.57	1.93:	2	1
22	15.31	0.70	0.24	-	1
29	15.42	0.69	0.24	-	1
33	15.57	0.67	0.19	-	1
49	15.43	0.67	0.22	-	1
57	15.83	0.72	0.16	-	1
70	15.50	0.71	0.25	-	1
96	15.51	0.65	0.16	-	1
102	13.28	0.55	0.01	1	-
108	15.58	0.72	0.22	-	1
117	12.49	0.68	0.13	1	2
125	16.32	0.76	0.29	-	1
135	14.98	0.53	-	4	-
136	12.30	0.61	0.03	7	7
137	12.76	0.56	-0.02	2	-
138	9.80	1.53	1.78	8	6
145	14.99	0.68	0.07	-	1
*146	14.62	0.74	0.28	1	-
149	15.33	0.83	0.44	-	1
151	14.21	0.55	0.12	1	-
152	14.31	1.12	1.37	1	-
155	16.14	0.75	0.28	-	1
159	16.96	0.90	-	-	1
160	17.60	1.06	-	-	1
161	17.00	0.89	-	-	1
162	17.20	0.94	-	-	1
163	17.41	0.74	-	-	1
Outside					
A	13.04	1.03	0.71	1	-
B	14.86	0.76	0.44	2	1
C	13.34	1.45	-	1	-
D	13.37	0.30	0.11	1	-
E	12.93	0.67	0.12	1	-
F	12.19	0.48	-0.01	1	1
G	8.18	0.25	0.14	1	-
H	8.69	0.95	0.69	1	-
I	12.72	0.53	0.06	1	-
J	10.88	1.41	1.45	1	1
K	14.66	0.60	-	1	-
L	12.50	1.23	1.16	1	1
M	8.91	0.11	0.17	1	-
N	10.79	0.59	0.21	1	-
O	7.95	0.96	0.70	1	-
P	13.00	0.45	-0.02	1	-
Anon	12.28	0.64	0.08	-	1
Anon	-	0.77	0.40	-	1

*Double Star. Measurement refers to combined light.

unknown systematic error is present, the accuracy of the final tabulated magnitudes of the five local standards should be high.

All photoelectric stars are identified in Figure 1, which is a reproduction of a 200-inch plate of 10-minute exposure taken on a 103*a*-D plate behind a GG11 filter. The scale of Figure 1 can be found from the size of the circles. Ring I has a diameter of 335″ of arc, ring II has a diameter of 670″, and ring III has a diameter of 1020″.

The first photographic plates were taken in January, 1958, at the Newtonian focus of the 60-inch reflector. The mirror was diaphragmed to 32 inches, to increase the size of the photometric field. Eastman 103*a*-O plates behind 2 mm of Schott GG13 filter were used for B magnitudes; Eastman 103*a*-D plates behind 2 mm of Schott GG11 filter were used for V magnitudes.

Four 60-inch plates in each color were measured to a limiting magnitude of $V = 17.5$ with an iris-diaphragm photometer in the fall of 1959. Van den Bergh's preliminary 1958 magnitudes were not used because the plates were remeasured to incorporate new photoelectric standards into the photometry. Measurements to fainter magnitudes were made on two plates in each color taken with the 200-inch telescope.

The photographic data for the program stars are given in Table 2, which includes values for the stars of Table 1. The standard stars are indicated by asterisks. Comparison of the stars in common in these two tables shows that, to within the accuracy of the data, no systematic difference is present and, therefore, that the photographic data are on the B, V system. Analysis of the data shows that the random probable error of the magnitudes in Table 2 is $0^m.020$ in V and $0^m.028$ in $B - V$. Details of the error determination are given in Appendix A.

The stars of Table 2 are identified in Figures 2 and 3. Figure 2 shows the central zone. Almost all single, uncrowded stars brighter than $V = 19$, $B = 20.2$ were photometered in this region. Figure 3 shows the stars in rings II and III.

The color-magnitude (C-M) diagrams resulting from the data are shown in Figures 4, 5, and 6. The photoelectric data alone are given in Figure 4. Normal points are plotted as open circles. They define the main sequence and its termination point. For values brighter than $V = 16.78$, the normal points were obtained from the photographic data; but for those fainter than $V = 16.78$, the normal points were obtained from the photoelectric data alone.

Figure 5 is the C-M diagram for the stars in the central zone of Figures 1 and 3 and shows the principal features of the cluster. The main sequence extends from $V = 14.9$ to at least $V = 19.0$ at the faint end. The color of the main-sequence break point, uncorrected for reddening, is $B - V = 0.66$. A subgiant and giant branch is evident in Figure 5, but the number of stars in ring I is not sufficient to define it very well. One very blue star, I-132, occurs at $V = 18.97$, $B - V = -0.16$. The apparent modulus of NGC 188 of $m - M = 11.10$, derived in the next section, requires that $M_v \simeq +7.9$ for this star if it is a member of the cluster. Since no white dwarfs are known to be so bright, either the star is an unknown type of intermediate white dwarf, or it is a foreground white dwarf with a normal M_v of about $+11$. A final feature of Figure 5 is the few stars above the main-sequence termination point between color indices 0.4 and 0.6. Based on the number of field stars expected at this latitude and apparent magnitude, the six stars present are probably field stars.

Figure 6 is the combined C-M diagram for stars in rings I and II. The subgiant and giant branch is very well defined, and its shape is similar to that of M67 (Johnson and Sandage 1955). The number of stars which appear brighter than the main-sequence termination point is increased by about a factor of 4 over that of Figure 5. Because this factor is the increase in area of rings I and II compared with ring I alone, it is reasonable to expect that most, or all, of these stars are field stars. A second very blue star, number II-91 at $V = 16.29$, $B - V = -0.17$, is present. Again, it appears likely that II-91 is a foreground white dwarf.

1962ApJ...135..333S

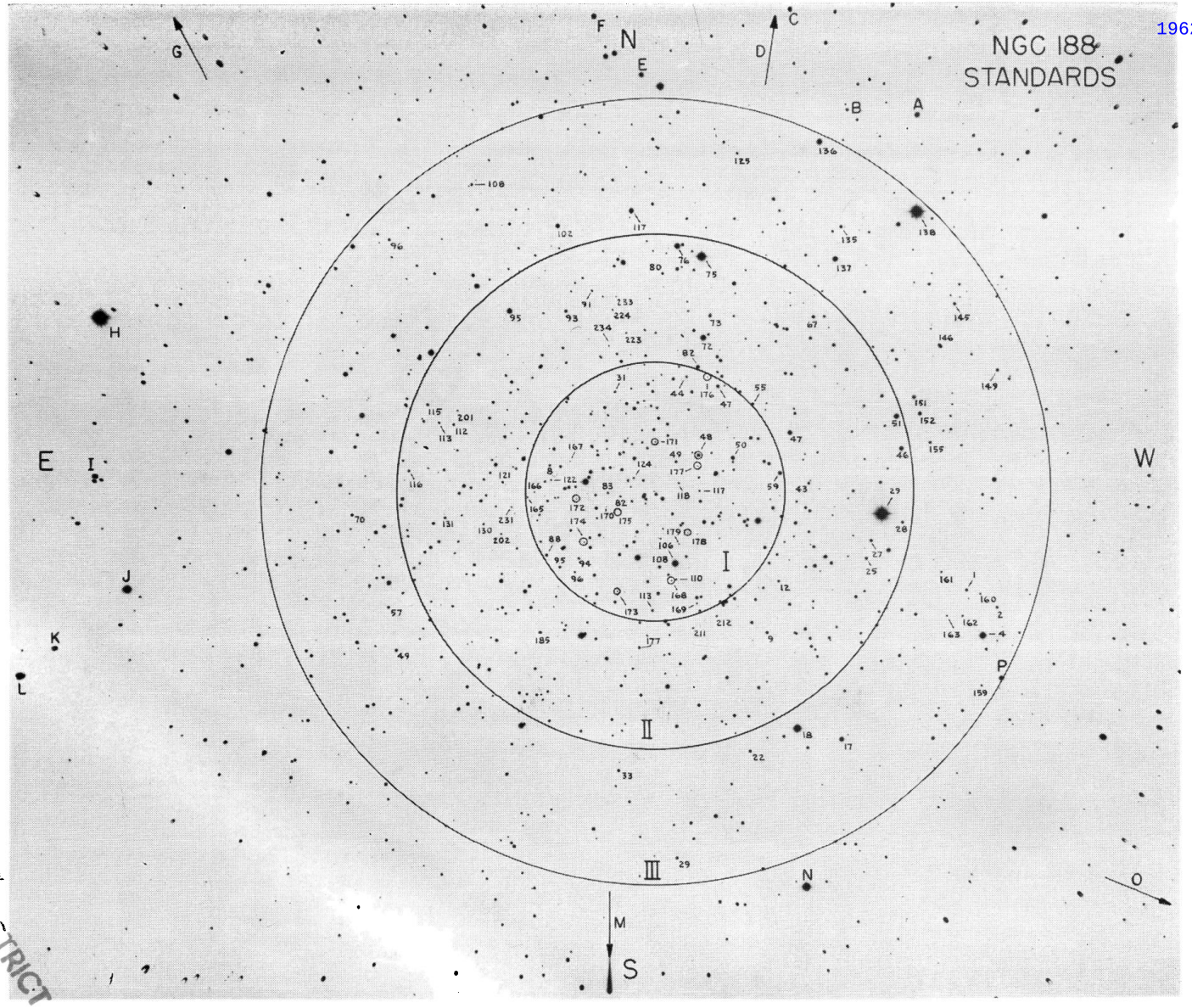

FIG. 1.—Identification chart for the photoelectric standards of Table 1. The reproduction is from a 10-minute photograph taken with the 200-inch telescope on an Eastman 103*a*-D plate behind a GG11 filter. The diameters of the three rings are 335, 670, and 1020 seconds of arc, respectively.

1962ApJ...135..333S

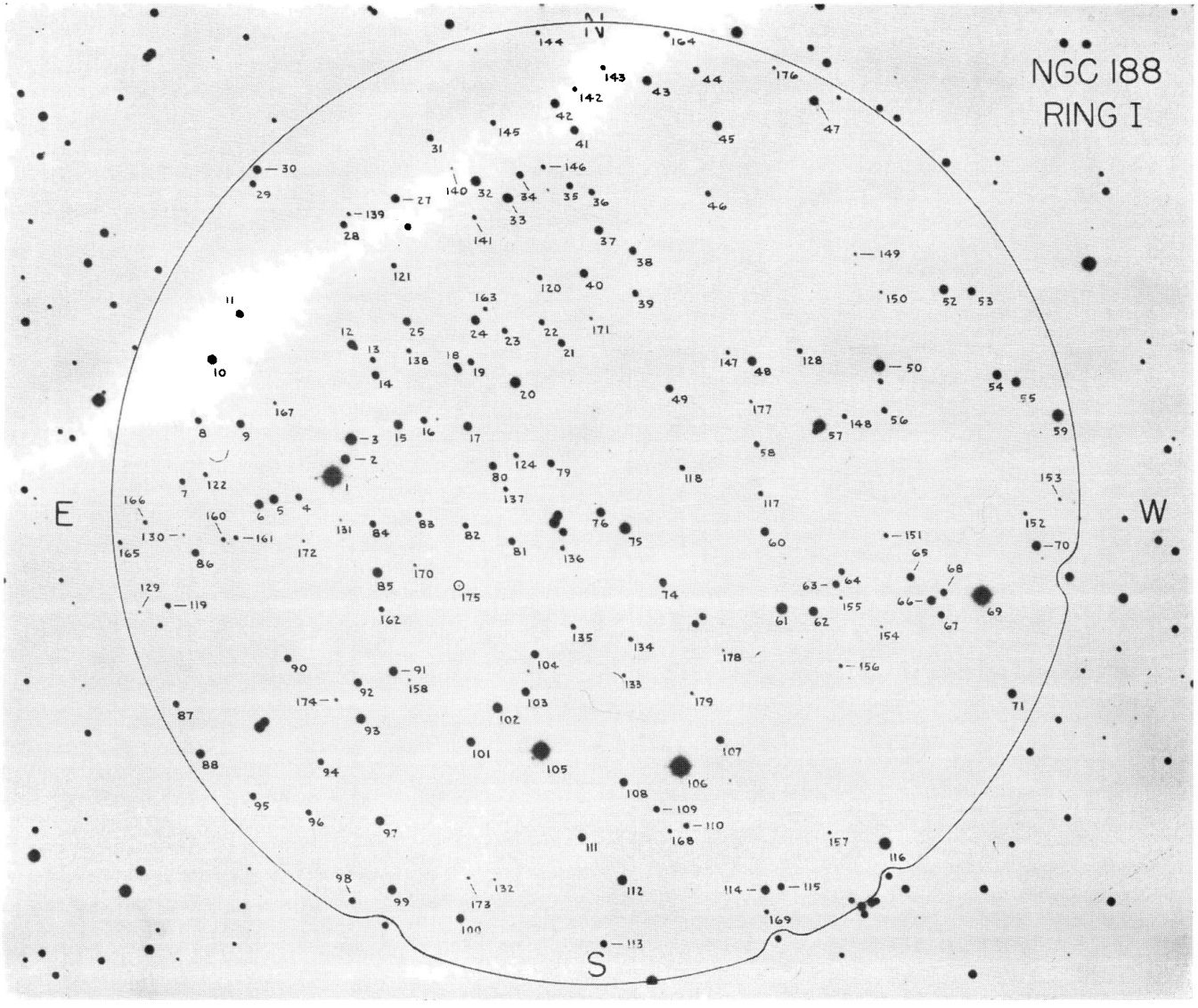

FIG. 2.—Identification chart for the stars in ring I of Table 2. The diameter of the circle is 335 seconds of arc. The print is from the same visual plate as in Fig. 1.

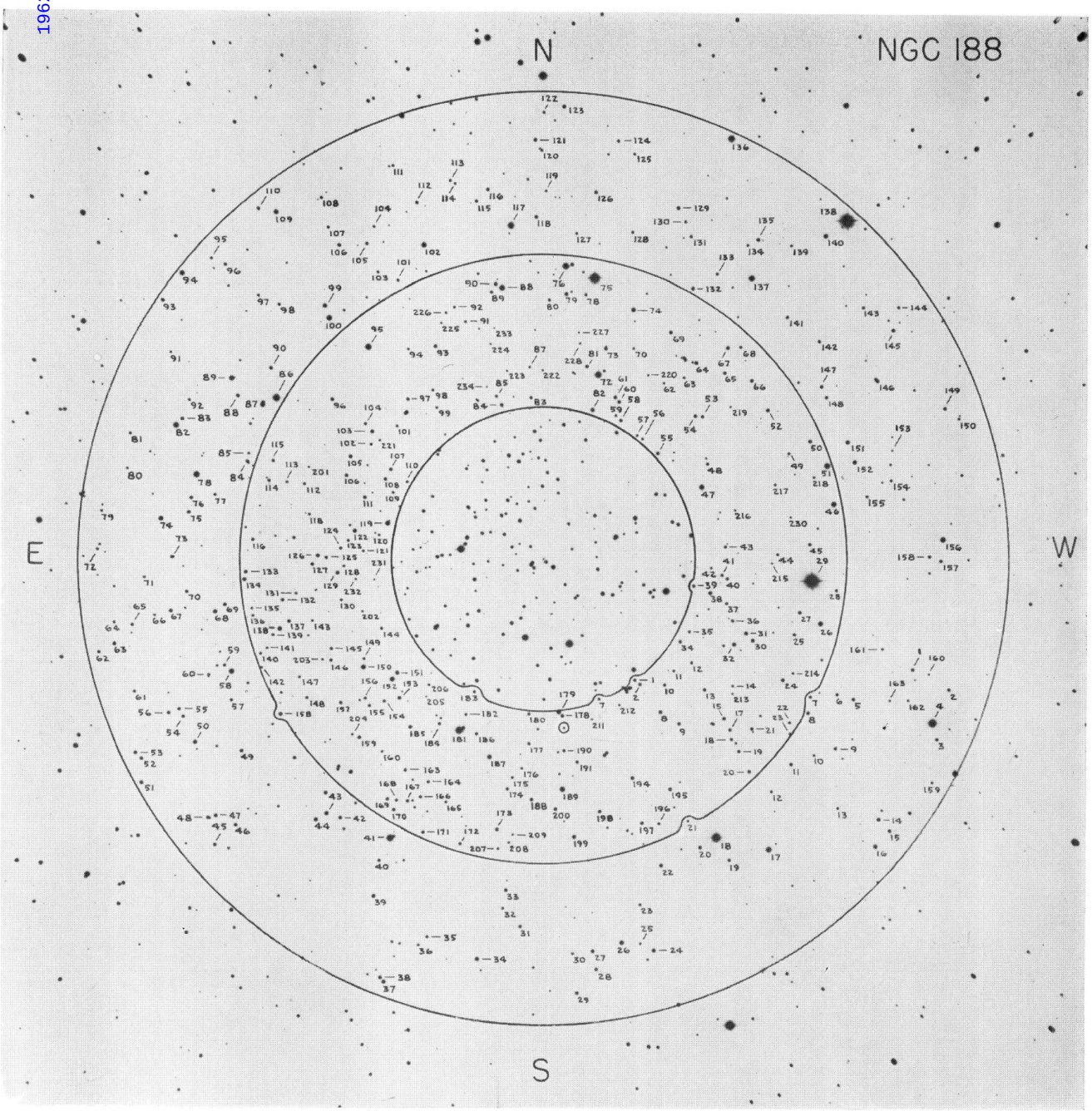

FIG. 3.—Identification chart for stars in rings II and III whose data are given in Table 2. The diameters of the circles are the same as in Fig. 1.

TABLE 2

DATA OBTAINED FROM PHOTOGRAPHIC PLATES

Star	V	B-V	Star	V	B-V	Star	V	B-V	Star	V	B-V
	Ring I					138	17.32	0.89	32	14.47	1.15
						139	18.15	1.25	33	16.46	0.65
1	11.93	1.18	68	15.86	0.80	140	19.38	1.29	34	15.69	0.51
2	14.53	0.86	69	12.26	1.34	141	17.71	1.19	35	16.36	0.77
3	13.90	0.50	70	14.88	0.72	142	17.90	1.10	36	15.75	0.72
4	16.32	0.81	71	15.11	0.61						
5	14.86	0.71	74	15.70	0.74	143	17.74	1.13	37	16.15	0.68
						144	17.99	1.29	38	14.77	0.59
6	14.85	0.98	75	13.81	1.16	145	17.04	1.06	39	15.06	0.69
7	16.71	0.87	76	15.01	0.70	146	17.60	0.93	40	15.60	0.67
* 8	16.50	0.80	79	15.89	0.62	147	17.94	1.02	41	15.75	0.67
9	15.50	0.84	80	15.51	0.71						
10	14.95	0.68	81	16.01	0.67	148	17.19	1.40	42	16.78	0.79
						149	18.88	0.67	* 43	15.88	0.73
11	16.12	0.94	* 82	16.80	0.84	150	18.95	1.06	44	16.02	0.77
12	15.01	0.75	* 83	16.75	0.90	151	17.65	0.99	45	15.52	0.64
13	16.85	-	84	16.21	0.85	152	18.23	1.14	* 46	13.40	0.46
14	15.47	0.66	85	14.62	1.06						
15	14.90	0.78	86	15.82	0.88	153	18.74	1.28	* 47	13.46	0.61
						154	19.28	1.64	48	15.83	0.69
16	16.05	0.83	87	16.36	0.89	155	18.68	1.08	49	16.40	0.69
17	15.11	0.65	* 88	15.04	0.94	156	18.28	1.18:	50	15.21	0.96
18	15.45	0.79	90	15.79	0.78	157	18.29	1.10	* 51	12.95	1.18
19	16.08	1.02	91	14.96	0.65						
20	14.28	0.88	92	15.51	0.70	158	19.21	-	52	14.93	0.74
						159	17.50	1.52	53	15.89	0.66
21	15.84	0.66	93	14.65	0.66	160	17.58	1.02	54	15.41	0.63
22	16.70	0.83	* 94	16.44	0.75	161	17.61	1.21	* 55	15.41	0.69
23	16.73	0.90	* 95	16.11	0.70	162	17.16	-	56	16.25	0.76
24	14.98	0.68	* 96	16.62	0.89						
25	15.38	0.65	97	14.99	1.00	163	17.91	1.04	57	16.48	0.89
						164	16.97	0.91	58	15.31	0.64
27	15.15	0.82	98	16.37	0.88	*165	17.63	1.03	59	16.65	0.71
28	16.04	0.68	99	14.95	0.70	*166	17.95	1.25	60	14.89	0.70
29	16.28	0.77	100	15.25	0.69	*167	18.52	0.91	61	15.12	0.69
30	15.28	0.72	101	15.14	0.64						
* 31	16.35	0.73	102	14.45	0.60	*168	17.80	0.96	62	16.88	0.87
						*169	17.69	0.85	63	16.61	0.75
32	14.52	0.59	103	15.19	0.62	*170	18.91	1.11	64	14.97	0.66
33	14.58	0.76	104	15.48	0.68	*171	18.67	1.13	65	15.34	0.70
34	15.84	0.78	105	12.32	1.25	*172	19.03	1.35	66	14.94	0.72
35	16.28	0.96	*106	11.91	0.47						
36	16.52	0.61	107	15.86	1.55	*173	18.74	0.72	* 67	14.94	0.69
						*174	18.62	1.41	68	16.35	0.50
37	15.30	0.68	*108	15.17	0.72	*175	19.96	-	69	15.20	0.59
38	15.37	0.70	109	16.31	0.77	*176	18.66	0.76	70	16.71	1.10
39	16.12	0.72	*110	16.86	0.83	*177	18.52	1.23	* 72	12.38	1.33
40	15.28	0.68	111	15.24	0.64						
41	15.31	0.70	112	14.49	0.71	*178	19.32	1.66	* 73	15.03	0.69
						*179	18.31	1.14	74	13.88	0.46
42	15.09	0.99	*113	16.05	0.77				* 75	(10.75)	(1.33)
43	15.02	0.56	114	14.84	0.65		Ring II		* 76	12.38	1.23
* 44	16.42	0.82	115	15.73	0.71				78	15.81	0.67
45	15.08	0.65	116	13.77	0.98	1	16.01	0.70			
46	16.64	1.02	*117	17.36	0.96	2	15.34	0.65	79	14.65	1.00
						7	16.22	0.76	* 80	15.78	0.66
* 47	15.03	0.70	*118	16.97	1.10	8	15.10	0.58	81	15.06	0.70
* 48	14.90	0.75	119	16.96	1.04	* 9	15.35	0.63	* 82	14.17	0.47
* 49	15.74	0.67	120	17.06	0.88				83	15.74	0.71
* 50	13.87	0.46	121	17.04	0.98	10	15.61	0.64			
52	15.00	0.63	*122	17.47	0.91	11	16.57	0.89	84	14.99	0.68
						* 12	16.19	0.77	85	16.15	0.87
53	15.79	0.75	123	17.06	1.05	13	15.27	0.44	87	16.73	1.08
54	15.05	0.69	*124	17.15	0.99	14	16.68	1.01	88	12.90	1.29
55	14.93	0.83	125	17.09	0.57				89	15.59	0.68
56	16.43	0.92	126	17.03	0.98	15	15.14	1.08			
57	13.55	1.18	127	17.49	1.00	17	15.93	0.69	90	14.78	0.87
						18	16.03	0.68	* 91	16.47	-0.37
58	16.83	0.75	128	16.97	1.01	19	15.86	0.53	92	16.51	0.84
* 59	13.95	1.05	129	19.41	0.61	20	15.25	0.58	* 93	14.97	0.85
60	15.26	0.63	130	19.30	0.88				94	16.90	0.95
61	14.12	1.12	131	19.28	1.36	21	15.80	0.63			
62	14.86	0.74	132	18.97	-0.16	22	16.54	0.80	* 95	12.55	0.76
						23	16.17	0.74	96	14.96	0.74
63	15.86	0.72	133	18.09	1.32	24	15.07	0.58	97	15.53	0.68
64	16.23	1.00	134	17.64	0.88	* 25	15.48	0.96	98	16.04	0.75
65	15.46	0.63	135	17.10	0.90				99	16.54	0.78
66	14.95	0.92	136	17.63	1.06	26	13.57	1.00			
67	16.06	0.72	137	17.48	0.89	* 27	15.25	0.66	101	16.74	0.79
						* 28	15.86	0.68	102	16.42	0.64
						30	15.03	0.99	103	14.92	0.65
						31	14.68	0.40	104	16.05	0.79
									105	15.02	0.54

TABLE 2 (cont'd)

Star	V	B-V
	Ring II (cont'd)	
106	15.58	0.64
107	15.08	0.68
108	15.18	0.61
109	16.41	0 76
110	16 11	0.76
111	15.24	1.34
*112	16.14	0.77
*113	16.52	0.77
114	15.87	0.92
*115	15.91	0.74
*116	16.06	0 76
118	16.57	0.64
119	13.47	0.45
120	16.56	0.88
*121	16.26	0.76
122	14.23	1 07
123	16.48	0.96
124	15 97	0.76
125	15.95	0.70
126	14.32	1.16
127	15.43	0.50
128	16.46	0.74
129	14.91	0.70
*130	16.72	0 80
*131	16.38	0.81
132	15.42	0.61
133	15.02	0.71
134	14.57	0 71
135	16.87	0.95
136	16.70	0.88
137	15.25	0.62
138	14.28	0.60
139	16.05	0.79
140	16.77	1.02
141	16.25	0.66
142	16.77	0 88
143	16.78	1.11
144	16.40	0.77
145	15.66	0.67
146	16.08	0.77
147	16.64	0.72
148	16.37	0.90
149	16.33	0.74
150	13.61	1.29
151	14.67	0.50
152	13.63	1.11
153	14.98	0.67
154	16.13	0.70
155	16.14	0.70
156	16.01	0.67
157	15.72	0.66
158	14.86	0.71
159	15.03	0.62
160	16.89	0.82
162	14.75	1.06
163	15 73	0.73
164	16.39	0.73
165	16.63	0 86
166	16.24	0.73
167	15.95	1.03
168	16.62	0.78
169	15.86	0.57
170	15.56	0.67
171	15.96	0.61
172	16.53	0.79
173	15.73	0.64
174	15.81	0.65
175	16.44	0.75
176	16.74	0.80
*177	16.08	0.77
178	13.91	1.19
179	15.00	0.68
180	16.15	0.70
181	12.09	1.24
182	16.71	0.79
183	16.33	0.77
184	15.91	0.76
*185	15.48	0.72
186	15.93	0.78
187	14 04	1.11
188	15.44	0.63
189	13.30	0 60
190	16.08	0.45
191	15.53	0.69
194	14.98	1.03
195	15.13	1.01
196	16.52	0.73
197	15.09	0.68
198	15.35	0.52
199	14.74	0.64
200	15.20	0 76
*201	17.50	1.00
*202	17.20	0.95
203	17.27	0.98
204	17 26	0 89
205	17.02	0.80
206	16.87	1 41
207	17.21	0.92
208	17 32	1.35
209	17 35	0 65
210	17.00	0.96
*211	17.35	0.93
*212	17.18	0 94
213	17.66	0.60
214	17.04	0.96
215	17.63	0 50
216	17.14	1.07
217	17.01	0.85
218	17.00	0.52
219	17.52	0.97
220	17.42	1.16
221	16 99	0.89
222	17.06	0.88
*223	17.51	0.97
*224	17 62	1.15
225	17.38	0.89
226	16.86	0.88
227	17.53	0.47
228	17.11	0.51
230	17.48	0 92
*231	17.81	0.98
232	17.08	0.98
*233	18.31	1.19
*234	17.95	1.38
	Ring III	
* 1	15.57	0.67
* 2	15.64	0.55
3	15.97	0.98
* 4	11.69	1.10
5	15 30	0.67
6	15.57	0.68
7	16.14	0.75
8	15.54	0.68
9	15.45	0.69
10	16.83	0.82
11	15.70	0.77
12	16.66	0.78
13	16.82	0.81
14	15.04	0.83
15	15.85	0.77
16	14.57	0.53
* 17	13.20	1.06
* 18	11.37	1.51
19	15.76	0.75
20	15.49	0.67
21	17.02	0.91
* 22	15.29	0.70
23	16.44	0.80
24	14.89	1.07
25	17.09	0.79
26	14.11	0.94
27	15.13	1.30
28	16.19	0.73
* 29	15.45	0.68
30	16.67	0.79
31	16.16	0.81
32	17.07	0.99
* 33	15.59	0.69
34	14.57	1.08
35	16.78	0.75
36	16.87	0.56
37	14.75	0.75
38	15.12	0.98
39	14.95	0.55
40	16.05	0.72
41	12.32	0 57
42	15.78	0.82
43	14.53	0.61
44	14.77	0.68
45	15.61	0.73
46	15.27	1 03
47	15.02	0.95
48	15.66	1.03
* 49	15.40	0.72
50	14.44	1.10
51	14.78	0.68
52	15.03	0.71
53	14.92	0.76
54	15.70	0.74
55	15.33	0.74
56	15.18	0.46
* 57	15.83	0.76
58	13.34	1.19
59	15.98	0.74
60	16.15	0.89
61	16.05	0.80
62	15.97	0.74
63	14.84	0.75
64	16.38	0 68
65	15.56	0.72
66	16.62	0.93
67	14.99	0.72
68	14.44	1.04
69	14.98	0.67
* 70	15.49	0.74
71	16.23	0.81
72	16.39	0.86
73	15.13	0.74
74	13.61	0.59
75	14.92	0.88
76	15.23	0.73
77	16.20	0.77
78	12.57	0.92
79	16.31	0.84
80	16.48	0.79
81	16.07	0.78
82	13.05	1.03
83	15.07	1.48
84	15.22	0.77
85	16.66	1.01
86	12.16	0.98
87	13.32	0.74
88	15.16	0.99
89	13.23	0.81
90	14.88	0.64
91	16.75	0.95
92	16.11	0.72
93	14.87	0.76
94	13.22	1.32
95	16.34	0.78
* 96	15.50	0.70
97	16.21	0.77
98	15.61	0.70
99	14.16	0.77
100	13.08	0.47
101	15.99	0.79
*102	13.24	0.57
103	16.18	0.77
104	16.60	0.91
105	15.36	0.73
106	14.81	0.67
107	15.82	0.88
*108	15.66	0 74
109	13.65	0.70
110	15.07	0.66
111	16 08	0.89
112	15.23	0.71
113	16.27	1.06
114	16.61	0.87
115	15.43	0.54
116	15.31	0.67
*117	12.51	0.68
118	15.06	0.71
119	16.61	0.74
120	16.29	0 54
121	14.94	0.84
122	16.06	0.88
123	14.58	0.82
124	15.73	0.65
*125	16.35	0.80
126	15.13	0.67
127	16.29	0.75
128	16.14	0.77
129	14.88	0.67
130	16.17	0.91
131	15.71	0.74
132	14.81	0.50
133	16.03	0.70
134	16.56	0.89
*135	15.02	0.53
*136	12.33	0.58
*137	12.75	0.54
139	16.46	0.66
140	13.92	1.09
141	15.88	0.65
142	15.87	0.69
143	15.93	0.66
144	16.21	0.89
*145	15.00	0.64
147	15.59	0.87
148	15.82	0.73
*149	15.35	0.79
150	16.35	0.76
*151	14.19	0.54
*152	14.37	1.07
153	17.42	0.22
154	16.49	0.77
*155	16.19	0.71
156	13.31	0.64
157	15.50	0.68
158	15.76	0.69
*159	17.05	0.86
*160	17.55	1.08
*161	16.99	0.82
*162	17.19	0.94
*163	17.46	0.71
	Outside	
*A	13.08	1.02
*B	14.93	0.80
*C	13.39	1.42
*D	13.34	0.33
*E	12.94	0.67
*F	12.18	0.48
*J	10.81	1.46
*K	14.67	0.60
*L	12.46	1.26
*N	10.83	0.50
*P	13.00	0.40

* Photoelectric standard in Table 1.

III. THE REDDENING, CHEMICAL COMPOSITION, AND DISTANCE MODULUS

The observed color index of the main-sequence termination point is $B - V = 0.66$, which is 0.17 mag. *redder* than the reddening-corrected termination point in M67. Therefore, the decision whether NGC 188 is older than M67 or not rests entirely with the reddening $E(B - V)$ of the NGC 188 stars. If $E(B - V)$ for NGC 188 is smaller than 0.17 mag., then the termination point of NGC 188 is intrinsically redder and the cluster is older than M67.

Figure 7 shows the $U - B$, $B - V$ diagram for the photoelectric stars of NGC 188 from Table 1. The solid line is the normal relation defined by Hyades stars (Eggen and Sandage 1959) from $B - V = 0.30$ to $B - V = 1.00$ and extended blueward and

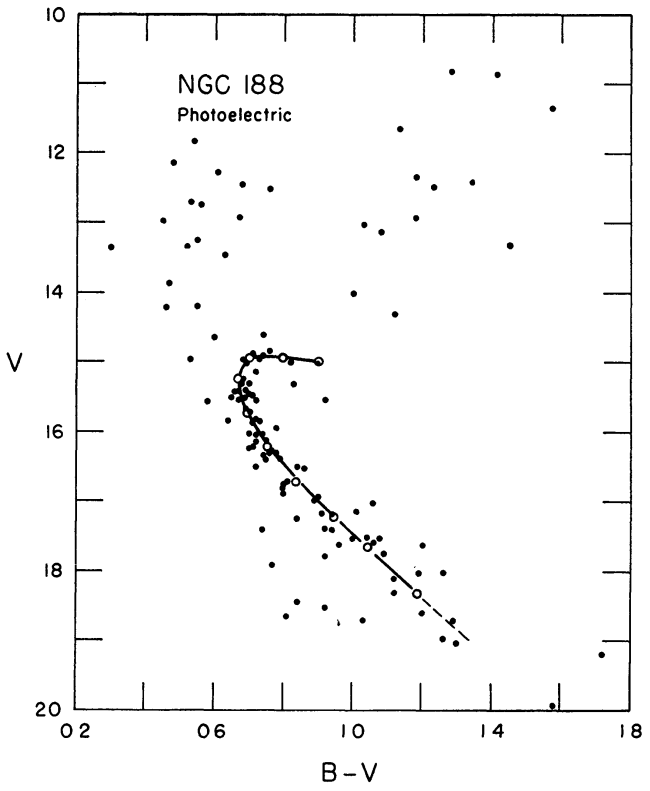

FIG. 4.—The color-magnitude diagram defined by the photoelectric standards of Table 1. The observed values are plotted, uncorrected for absorption and reddening. Normal points taken from Table 4 are shown.

redward by Table 14 of Johnson and Morgan (1953). Most of the stars in Figure 7 bluer than $B - V = 0.66$ are field stars (see Fig. 4) and tell nothing about the reddening of the cluster. Nearly all stars redward of $B - V = 0.66$ are cluster members and are used to determine the reddening by the three-color method.

The three-color method applies only if the stars in question have the same chemical composition as those in the Hyades. If stars in NGC 188 have a lower metal abundance, then they will certainly show an ultraviolet excess relative to Hyades stars due to a smaller line blanketing. This excess will imitate the effect of interstellar reddening because the U, B, V system cannot separate the two effects for F and G stars for small $E(B - V)$ or $\delta(U - B)$ values. Therefore, the reddening determined from Figure 7 remains ambiguous until the chemical composition of the stars in NGC 188 is known.

An upper bound can be put on $E(B - V)$ as follows: If the stars have the Hyades metal abundance, then the deviation of the points from the line in Figure 7 is due entirely to reddening and $E(B - V) = 0.05$ mag. On the other hand, $E(B - V)$ could be zero if the stars in NGC 188 have weak Fraunhofer lines which produce an ultraviolet excess of $\delta(U - B) \simeq 0.06$ mag. A third highly unlikely possiblity is that the metal abundance of stars in NGC 188 is so much higher than that of the Hyades stars that the normal $U - B$, $B - V$ line lies *below* that of Figure 7. In this case, the value of $E(B - V)$ would have to be greater than 0.05 mag. to produce the observed deviation of the points in Figure 7. The great age of NGC 188 makes an abnormally high metal abundance improbable. Therefore, $E(B - V)$ probably lies between 0.00 and 0.05 mag., depending upon the chemical composition.

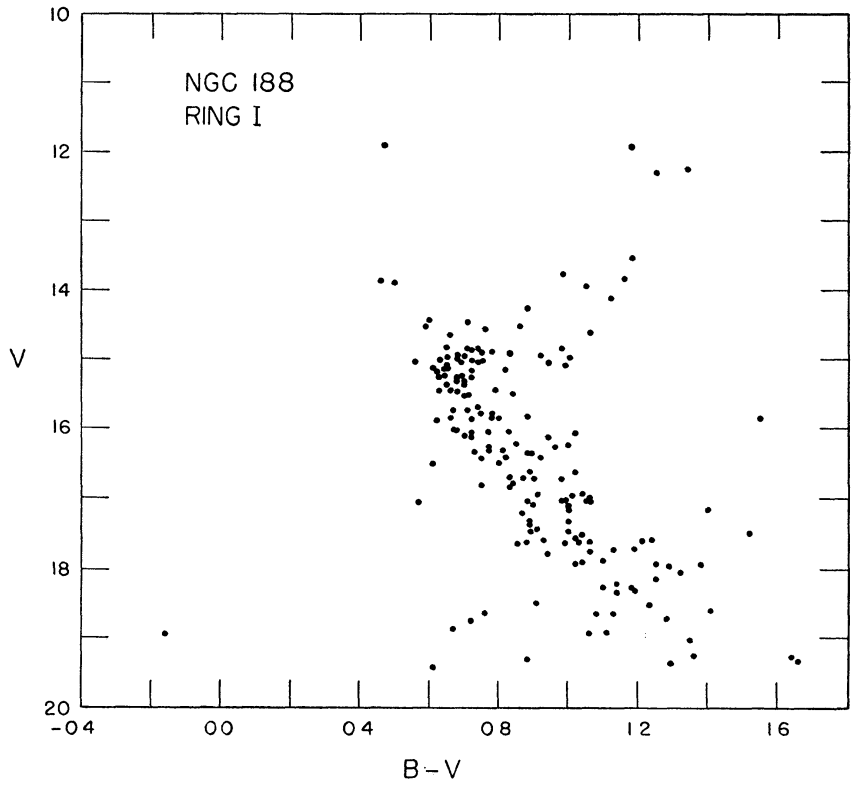

FIG. 5 —The color-magnitude diagram for the stars in the central zone The data are from Table 2. No reddening or absorption corrections are applied All uncrowded, single stars in ring I have been measured and are shown here.

To settle the question, spectra were taken of four stars near the main-sequence termination point in NGC 188. The stars are faint and required long exposure times at the prime-focus grating spectrograph of the 200-inch telescope. The spectra were widened sufficiently for classification at a dispersion of 180 A/mm. Spectra of several classification standards were taken with the same instrument during the same observing period. Dr. Philip Keenan kindly classified the spectra, and his results are shown in Table 3. The types of all four stars were early G, with no evidence of line weakening, but the dispersion was so small that this conclusion is not firm. These data therefore suggest, but do not prove, that the stars in NGC 188 have a normal metal abundance. The reddening determined from the spectral data is $E(B - V) = 0.052 \pm 0.02$ mag., which agrees well with $E(B - V) = 0.05$ mag from the three-color data, assuming normal

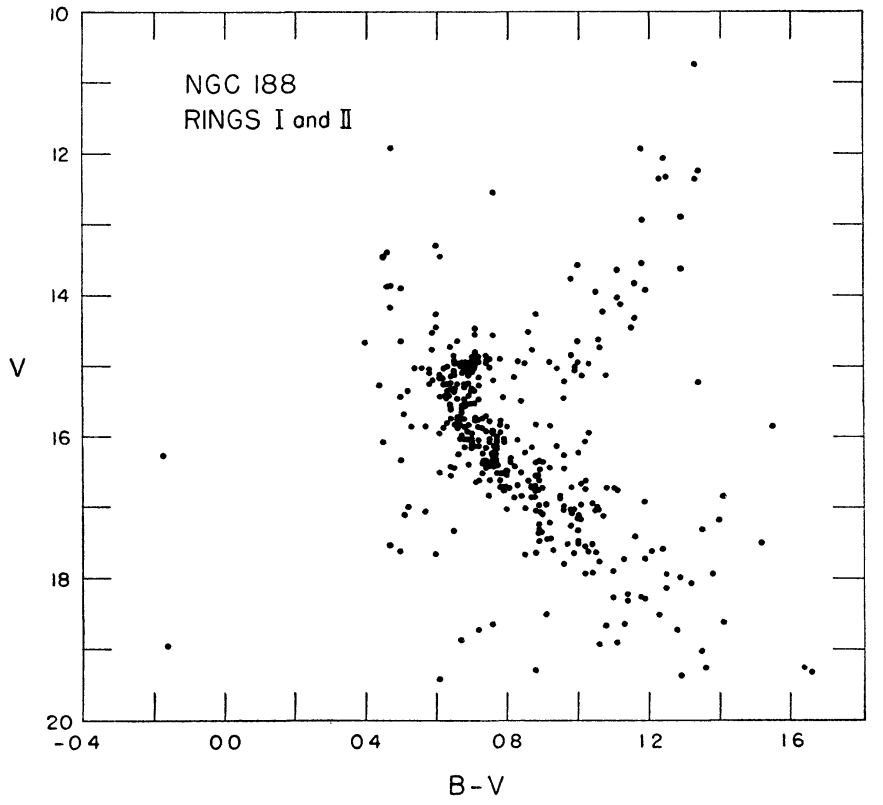

FIG. 6.—Same as Fig. 5 for rings I and II

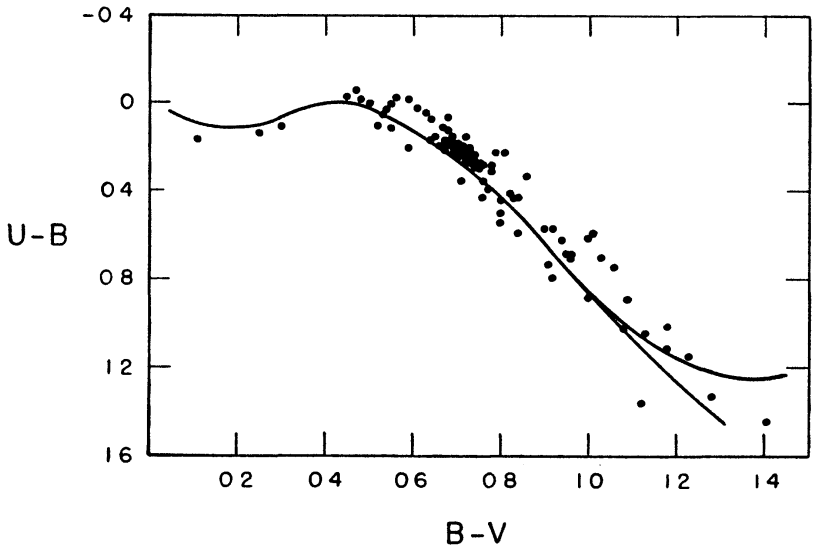

FIG. 7.—The $U - B$, $B - V$ diagram for the photoelectric stars of Table 1. The line is the unreddened relation for Hyades stars.

chemical composition. We adopt $E(B-V) = 0.05$ mag. in what follows and assume that the chemical composition of the stars in NGC 188 is the same as for the Hyades.

Normal points obtained from the photometric data are given in the first two columns of Table 4. The normal points corrected for reddening are tabulated in columns 3 and 4. The main-sequence section of these columns was then used to determine the modulus as follows.

The age-zero Hyades main sequence (Sandage 1957) was used as the standard unevolved sequence. The photometry has not been carried faint enough in NGC 188 to reach completely unevolved stars, and the effects of evolution must be computed to obtain $m - M$. This can be properly done only if tracks of evolution are available in the M_v, $B-V$ plane over the entire relevant mass range (1 $\mathfrak{M}\odot$ to about 0.7 $\mathfrak{M}\odot$). In lieu of these extensive and unavailable data, we assume homology over the range of 4 mag. from $M_v = +4$ to $M_v = +8$ and adopt the single evolutionary track computed

TABLE 3

SPECTRAL DATA ON NGC 188

Star	V	$B-V$	Sp	$(B-V)_0$	$E(B-V)$
II-2	15 34	0 65	G1 V_p	0 62	0 03
II-27*	15 29	68	G3 V_p	65	03
II-73*	15 03	69	G2 V	64	05
II-96	14 96	0 74	G2 V	0 64	0 10
					0 052±0 02 (A.D.)

* V and $B-V$ are photoelectric values

TABLE 4

NORMAL POINTS FOR NGC 188 SEQUENCES

V (1)	$B-V$ (2)	V_0* (3)	$(B-V)_0$* (4)	M_{v0} (5)	B C. (6)	M_{bol} (7)	log T_e (8)
11 50	1 50	11 35	1 45	0 40	. . .	. .	
12 00	1 36	11 85	1 31	0 90	−0 95	−0 05	
12 50	1 28	12 35	1 23	1 40	−0 78	0 62	
13 00	1 21	12 85	1 16	1 90	−0 64	1 26	
13 50	1 16	13 35	1 11	2 40	−0 54	1 86	
14 00	1 12	13 85	1 07	2 90	−0 49	2 41	
14 50	1 08	14 35	1 03	3 40	−0 44	2 96	.
14 85	1 05	14 70	1 00	3 75	−0 40	3 35	3 666
15 02	1 00	14 87	0 95	3 92	−0 33	3 59	3 675
15 00	0 90	14 85	0 85	3 90	−0 22	3 68	3 696
14 97	0 80	14 82	0 75	3 87	−0 15	3 72	3 723
14 97	0 699	14 82	0 649	3 87	−0 09	3 78	3 752
15 29	0 664	15 14	0 614	4 19	−0 07	4 12	3 762
15 75	0 696	15 60	0 646	4 65	−0 09	4 56	3 752
16 23	0 758	16 08	0 708	5 13	−0 12	5 01	3 734
16 78	0 837	16 63	0 787	5 68	−0 17	5 51	3 713
17 24	0 946	17 09	0 896	6 14	−0 27	5 87	3 685
17 63	1 044	17 48	0 994	6 53	−0 39	6 14	3 665
18.31.	1 187	18 16	1 137	7 21	−0 59	6 62	3 645
(19 00)	(1 34)	(18 85)	(1 29)	(7 90)	−0 91	(6 99)	(3 610)
(19 50)	(1 44)	(19 35)	(1 39)	(8 40)	−1 17	(7 23)	(3 577)

* $E(B-V) = 0\ 05$; $A_v = 0\ 15$; $(m-M)_0 = 10\ 95$ assumed

by Hoyle (1959) for a star of mass 1.09 $\mathfrak{M}_\odot$. The detailed track and the predicted C-M diagrams which result are given in the following paper. The transformation of the computation from the M_{bol}, log T_e plane to the M_v, $B - V$ diagram is also discussed there. The distance moduli determined from these calculations are $(m - M)_0 = 10.95$ for NGC 188 and $(m - M)_0 = 9.58$ for M67. Column 5 of Table 4 gives the resulting M_{v0} for the normal points of NGC 188. Columns 6, 7, and 8 give the adopted bolometric corrections, M_{bol}, and log T_e—the latter for main-sequence stars only.

Figure 8 shows the fit of M67 and NGC 188 to the unevolved main sequence by using this procedure. The sun is shown for comparison, using Stebbins and Kron's (1957) apparent magnitude of $V = -26.73$ and $B = V - 0.63$. Several features of Figure 8

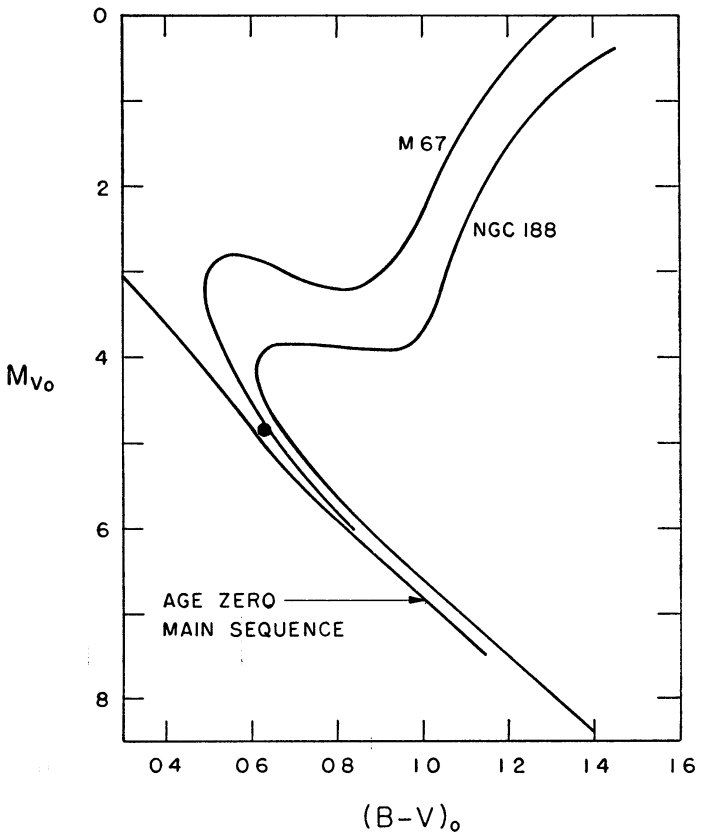

FIG. 8.—The fit of M67 and NGC 188 to the age-zero main sequence. The effect of initial evolution away from the main sequence has been considered. The M67 and NGC 188 diagrams have been corrected for absorption and reddening. The position of the sun is shown by a filled circle.

should be noted: (1) The main-sequence termination point for NGC 188 is about 1 mag. fainter than that of M67, assuming that $E(B - V) = 0^m.05$ for NGC 188 and $E(B - V) = 0^m.06$ for M67. (2) The shapes of the subgiant and giant branches of M67 and NGC 188 are nearly parallel, which suggests that homologous tracks of evolution in this part of the M_v, $B - V$ plane may be adequate. (3) Stars in NGC 188 must be older than the sun. Indeed, the data suggest that NGC 188 is the oldest galactic cluster yet found.

Confirmatory evidence for this conclusion comes from spectral data. If Figure 8 is correct, then the spectral types of stars at the M67 main-sequence termination must be 0.4 of a spectral class earlier than stars at the corresponding point in NGC 188. The check was made by taking spectra of six stars in M67 on the same nights that the spectra of the NGC 188 stars were obtained. The dispersion was again 180 A/mm,

and the quality of the spectrograms of the two clusters was comparable in every way. Table 5 gives Keenan's spectral types, together with the identifying number and the V magnitude given by Johnson and Sandage (1955). The mean type for the group is F9. The mean type for the four stars in NGC 188 is G2 (see Table 3). This check, which shows a difference of 0.3 of a spectral class, is considered satisfactory, and the conclusion remains that NGC 188 is older than M67.

IV. COMPARISON OF NGC 188 WITH OTHER AGGREGATES

Is NGC 188 as old as the field stars in the solar neighborhood? How does it compare with the globular clusters in the halo? Figure 9 shows the NGC 188 diagram superposed on O. C. Wilson's C-M diagram for the field stars (Wilson 1959). The schematic line for NGC 188 is within 0.2 mag. of the lower envelope of the field stars in the subgiant and giant regions. This requires that the age of the oldest field stars near the sun be about 1.2 times the age of NGC 188.

One important fact which emerges from Wilson's data is that the field stars near the lower envelope of the subgiant and giant regions have no detectable line weakening in their spectra despite their great age, i.e., these stars and the stars in NGC 188 appear to have a nearly normal (Hyades-like) abundance of the heavy elements. The present

TABLE 5

SPECTRAL TYPES FOR SIX STARS IN M67

Star	V	Type	Star	V	Type
83	13 24	F9	132	13 11	G0
94	12 81	F9	147	13 27	G0
127	12 78	F8	225	13 10	F8

data then require that *in the disk of the Galaxy near the sun there has been no appreciable enrichment of the heavy-element content in the time since the oldest galactic clusters were formed.* This conclusion affects certain current theories of element synthesis, and all possible observational tests, such as U, B, V photometry of the field stars near the lower envelope to detect an ultraviolet excess, should be made to check the data.

A comparison of NGC 188 with M67 and with three halo globular clusters is shown in Figure 10. Data for the three globular clusters were taken from Arp and Johnson (1955) and from Baum *et al.* (1959) for M13; from Johnson and Sandage (1956) for M3 (photoelectric data only); and from Arp (1962) for M5. Blanketing corrections have been applied to the measured colors of main-sequence, subgiant, and giant stars following the method of Sandage and Eggen (1959) as refined by Wildey *et al.* (1962). Normal points for the C-M diagrams of the globular clusters are given in the following paper (Sandage 1962). The adopted moduli and the absolute magnitudes of the main-sequence termination point M_v (T.P.) of the five clusters are given in Table 6. The M_v (T.P.) values are approximate because the termination point is a matter of more or less arbitrary definition.

The moduli and therefore the placements of the clusters in Figure 10 are valid only to the extent that the adopted age-zero main sequence is correct for five clusters (after blanketing corrections are applied to the globular clusters). This condition implies that the main sequences of the clusters are identical in the log T_e, M_{bol} plane, even though their chemical compositions differ. The computations of Hazelgrove and Hoyle (1959) support this requirement to within 0.1 mag., and the observational data for mild subdwarfs, corrected for blanketing (Sandage and Eggen 1959), confirm that a difference, if it exists, is smaller than 0.2 mag. for most stars.

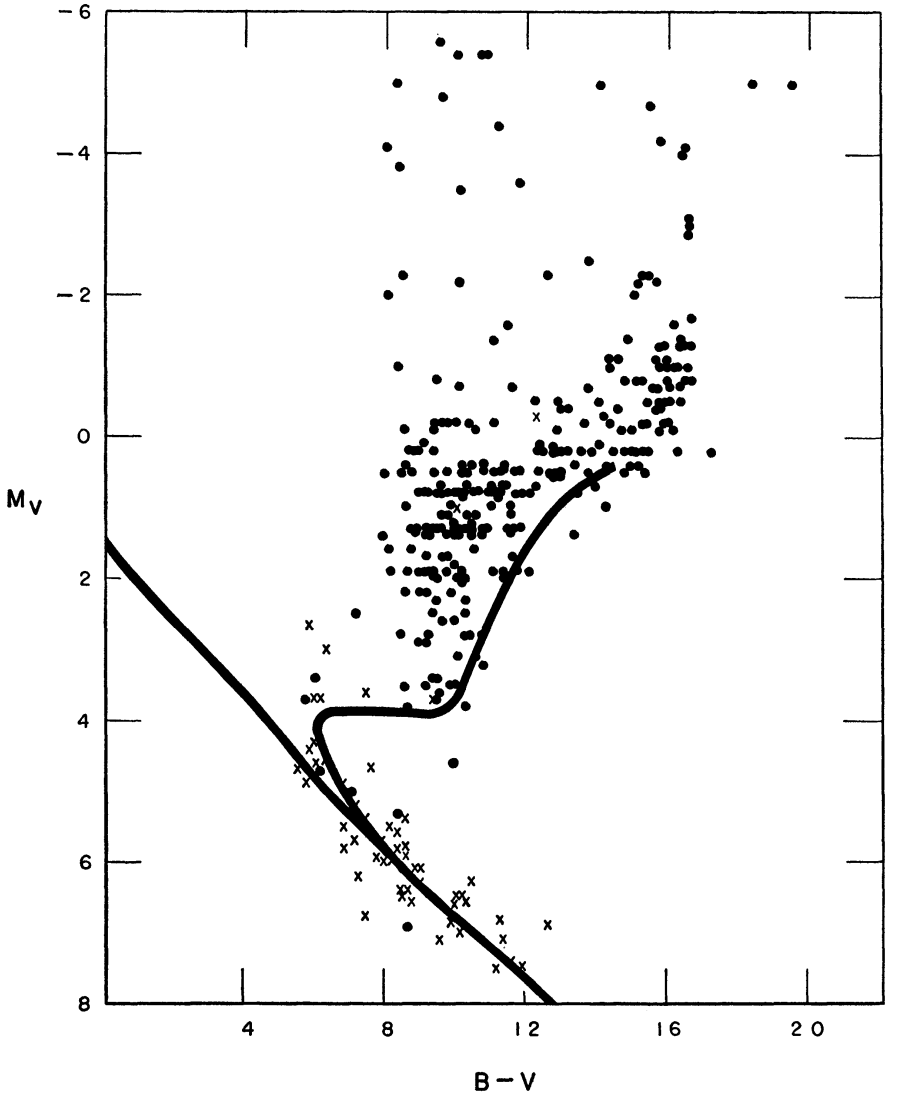

FIG. 9.—Comparison of the NGC 188 diagram with that of the nearby field stars after O. C. Wilson. The NGC 188 sequences have been corrected for absorption and reddening. NGC 188 is almost the lower envelope of the subgiant and giant field stars. The crosses represent stars with trigonometric parallaxes.

TABLE 6

ADOPTED MODULI AND TERMINATION POINT FOR FIVE CLUSTERS

Cluster	$(m-M)_0$	M_v(T P)	Cluster	$(m-M)_0$	M_v(T P)
M67. . .	9 58	3 0	M5.	14 30	4 1
NGC 188	10 95	4 1	M13	14 43	3 9
M3 .	14 60	4 2			

Several features of Figure 10 should be noted. (1) The main-sequence termination point occurs at about the same M_v for NGC 188 and for the three globular clusters. (2) The relative positions of the subgiant and giant sequences in the three globular clusters differ slightly from each other, presumably because of age and chemical composition differences. (3) The M_v of the brightest giants in globular clusters varies from -2.6 for M13 to -2.0 for M3. (4) The absolute magnitudes of the RR Lyrae stars are $M_v \simeq +0.3$ for M13, $M_v \simeq +0.8$ for M5, and $M_v \simeq +1.0$ for M3—values which are fainter than the traditional value of 0.0. These fainter numbers support the data given by Eggen's moving-group method applied to RR Lyrae itself (Eggen and Sandage 1959). More data of the same type for additional globular clusters are urgently needed before the calibration problem of the RR Lyrae stars can be considered well in hand.

Many people have helped with the present investigation. I wish to thank Dr. Ivan King for first telling me of the cluster, Dr. van den Bergh for his interest in measuring the first photographs, Mr. Frank Brueckel for help in the reduction and for his analysis

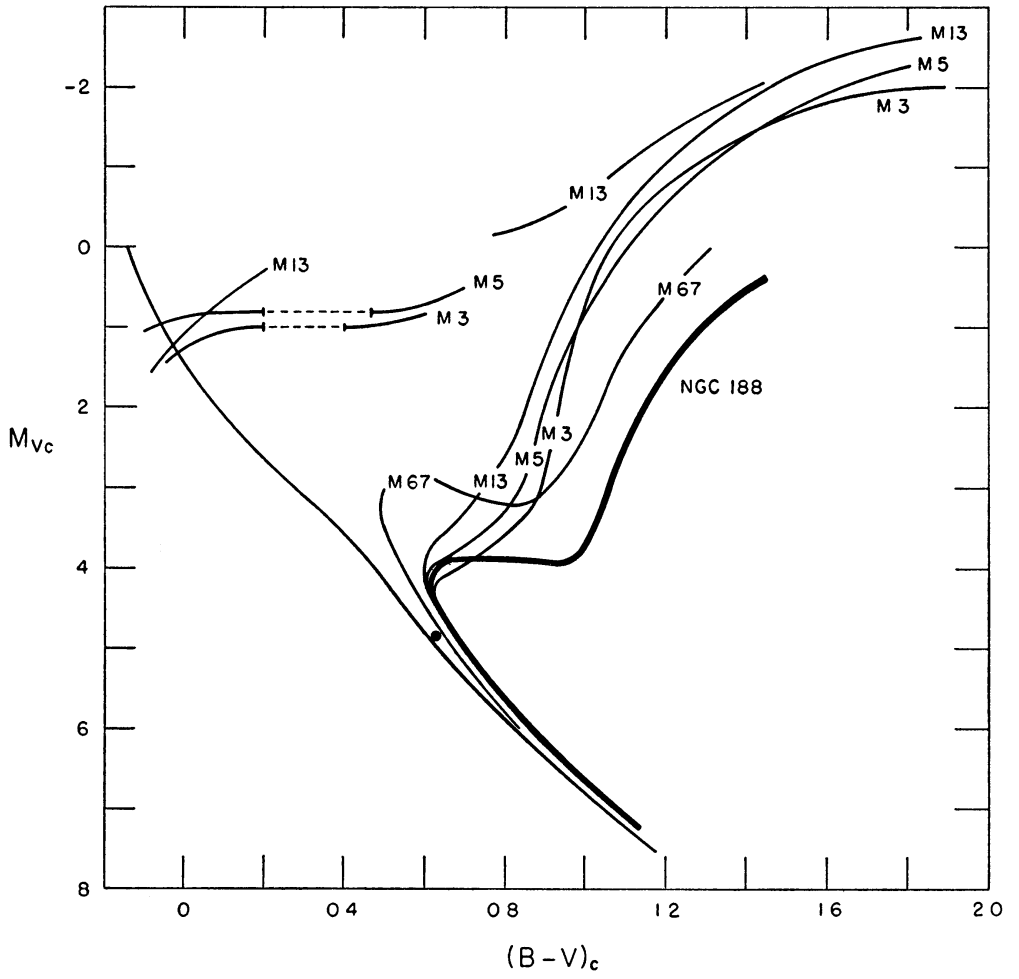

FIG. 10.—Comparison of the color-magnitude diagrams of M67, NGC 188, M3, M5, and M13. M67 and NGC 188 have been corrected for absorption and reddening. The three globular clusters have been corrected for the effects of differential line blanketing on the colors and magnitudes. The ordinate and abscissa are labeled with a subscript c to indicate corrected values. The main-sequence data for M3 are subject to revision.

of the residuals, my wife Mary for her help in the preparation of Table 2, Dr. Philip Keenan for his classification of the spectrograms, and Dr. H. C. Arp for checking several photoelectric stars with the 200-inch and for obtaining several of the first photographic plates with the 60-inch telescope. Finally, it is a pleasure to thank Miss Eileen Challacombe for her characteristically fine work in preparing the diagrams for press.

APPENDIX A

Analysis of the Random Photometric Errors

The random errors of photometry for stars in Tables 1 and 2 have been investigated in two ways.

1. The residuals of each of the four values of V and of B from the mean magnitudes in Table 2 were analyzed. These data provide nearly 2000 residuals in each color. Figure A1 shows the histogram for the distribution of the residuals of V magnitudes from the mean, for the program stars brighter than $V = 17.5$ measured on the 60-inch plates. The distribution satistactorily approximates a Gaussian, with $\sigma = 0.061$ mag. The full curve of Figure A1 is a normal distribution with the same area and dispersion as the histogram. Results for B magnitudes give a similar distribution, with $\sigma = 0.058$ mag. Therefore, the probable error of a single measurement of magnitude on the 60-inch plates is $0^m.041$ for V and $0^m.039$ for B. Because four independent measurements were made in each color, the random probable error of the tabulated magnitudes of Table 2 is $0^m.020$ for V and for B, and, because B and V are independent, the random probable error of $B - V$ is $0^m.028$.

2. An independent estimate is provided by comparison of Tables 1 and 2. No systematic difference appears to exist between the tables, which means that no color or magnitude equation is

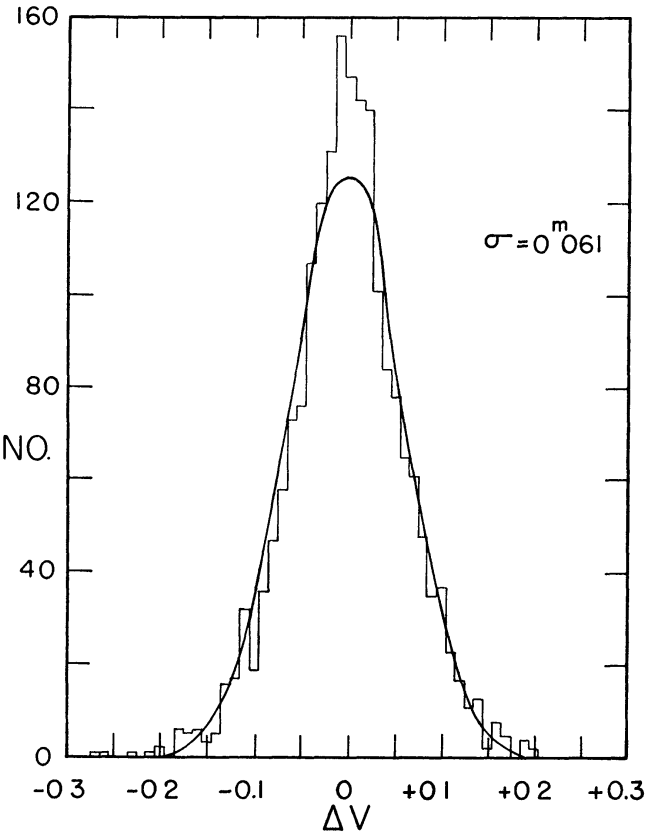

Fig. A1.—Histogram of the residuals of the four measured V magnitudes for each star from the means of Table 2 The line is a normal error distribution with the same area and dispersion as the histogram.

present larger than the error of the determination. The differences between Tables 1 and 2 are therefore due to the random errors. Analysis of the 96 residuals for stars brighter than $V = 17.6$ gives $\sigma = 0^m.042$ for the distribution of ΔV, $\sigma = 0^m.054$ for the distribution of $\Delta(B - V)$, and therefore $\sigma = 0^m.038$ for ΔB if B and V are independent. These dispersions are compounded of both the photographic and the photoelectric errors. If we assume $\sigma = 0^m.01$ for the random dispersion of the photoelectric data of Table 1, then $\sigma = 0^m.041$ for the V, and $\sigma = 0^m.037$ for the B value tabulated in Table 2. These give probable errors of $0^m.028$ for V and $0^m.025$ for B in Table 2, which are in satisfactory agreement with the results of the first method.

APPENDIX B

Comparison with the Photometry of Barkhatova

NGC 188 has been studied by the Soviet astronomer K. A. Barkhatova (1956) with plates taken with a 15-inch Schmidt telescope of the Engelhardt Observatory. Magnitude standards were obtained by photographic transfers from the N.P S. and from Selected Area 39. Barkhatova concludes from her color-magnitude diagram that NGC 188 has main-sequence stars as blue as CI = −0 31, corresponding to spectral type B7, and that NGC 188 resembles the young cluster NGC 2194 (Cuffey 1943). These results are so different from ours that a comparison of the two studies is necessary.

There are 90 stars in common between Table 2 and a magnitude list published by Mrs. Barkhatova. Comparison of the lists showed that differences of 1.5 mag. and more exist for some stars. Detailed comparison showed that the most discrepant stars are within 15 seconds of arc of other stars of comparable brightness. Furthermore, the magnitudes of these stars in Table 2 were always fainter than given by Barkhatova, which suggests that crowding difficulties were encountered with the Engelhardt material.

The comparison for non-crowded stars showed considerably better agreement, as Figure B1

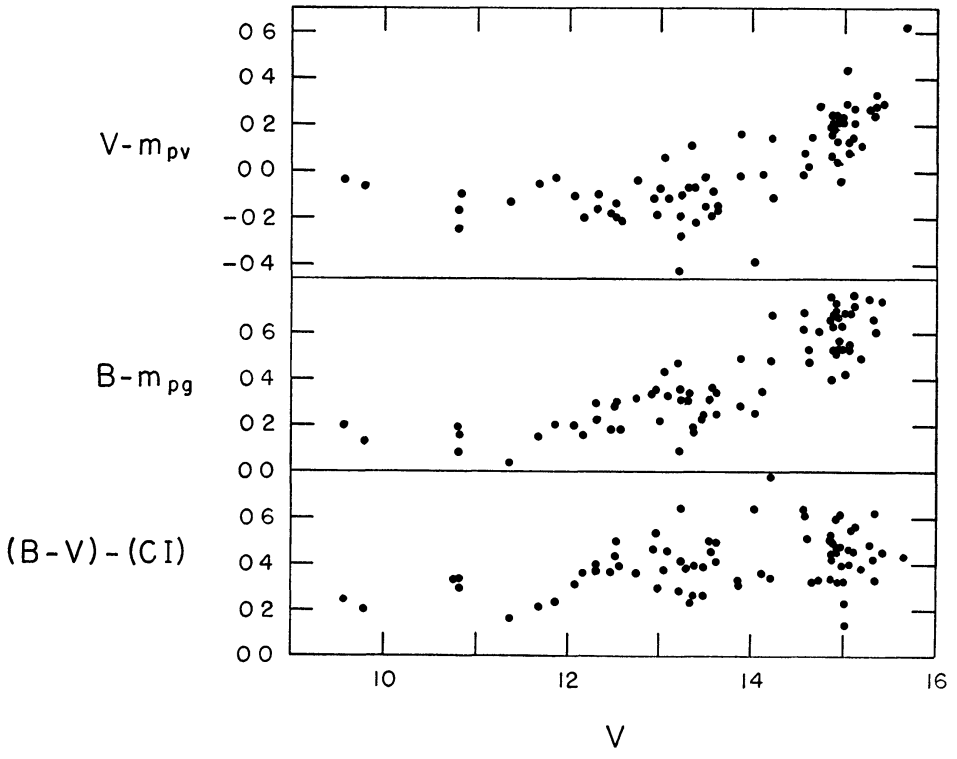

Fig B1.—Comparison of K A. Barkhatova's magnitudes with those of Table 2 of the present paper for 76 uncrowded stars in common The abscissa is V magnitude from Table 2 The ordinate gives the magnitude and color differences between the two studies.

indicates. The magnitude and color differences are plotted against the V magnitude of Table 2. A zero-point difference of $\Delta V \simeq -0^{m}13$ is present from $V = 10$ to $V = 13.5$, at which point a scale difference begins, which grows to 0.4 mag. at $V = 15.3$. The large-scale difference in $B - V$ is pronounced over the entire range of the comparison.

These photometric differences, serious as they are, do not entirely account for the difference in the topology of the C-M diagrams. Most of the stars measured by Barkhatova are outside the central region of the cluster. Quoting directly from her paper: "Difficulty was encountered in the photometry because of the high congestion of the stars of this cluster, which is exceptionally rich in faint stars, particularly in the central condensation, thus stars in the central region could not be measured." Because the data of the present paper show that the number of stars which fall off the principal sequences, and therefore presumed to be field stars, increases from ring I to ring III; because Barkhatova's data extend to twice the diameter of our ring III; and because only nine stars from the center of the cluster (our ring I) were measured, it seems probable that many of the stars in Barkhatova's list do not physically belong to NGC 188. If so, a spurious C-M diagram was obtained by Barkhatova.

REFERENCES

Arp, H. C. 1962, *Ap. J.*, **135**, 311.
Arp, H. C., and Johnson, H. L. 1955, *Ap. J.*, **122**, 171.
Barkhatova, K. A. 1956, *Russian A.J.*, **33**, 850.
Baum, W. A., Hiltner, W. A., Johnson, H. L., and Sandage, A. R. 1959, *Ap. J.*, **130**, 749.
Cuffey, James. 1943, *Ap. J.*, **97**, 93.
Eggen, O. J., and Sandage, A. R. 1959, *M.N.*, **119**, 255.
Hazelgrove, C. B., and Hoyle, F. 1959, *M.N.*, **119**, 112.
Hoyle, F. 1959, *M.N.*, **119**, 124.
Johnson, H. L., and Morgan, W. W. 1953, *Ap. J.*, **117**, 313.
Johnson, H. L., and Sandage, A R 1955, *Ap. J.*, **121**, 616.
———. 1956, *ibid.*, **124**, 379.
Sandage, A. 1957, *Ap. J.*, **125**, 435.
———. 1962, *ibid.*, **135**, 349.
Sandage, A. R., and Eggen, O. J. 1959, *M.N.*, **119**, 278.
Stebbins, J., and Kron, G. E. 1957, *Ap. J.*, **126**, 266
Wildey, W. L., Burbidge, E. M., Sandage, A R., and Burbidge, G. R. 1962, *Ap. J.*, **135**, 94.
Wilson, O. C. 1959, *Ap. J.*, **130**, 496.